COMPOSITES & POLYCON 2009
American Composites Manufacturers Association
January 15-17, 2009
Tampa, FL USA

Behavior of FRP Tubes-Encased Concrete Columns under Concentric and Eccentric Loads

by
Hamdy Mohamed, Department of Civil Engineering, University of Sherbrooke
Radhouane Masmoudi, Department of Civil Engineering, University of Sherbrooke

Abstract

Recently, Concrete filled fiber-reinforced polymers (FRP) tube (CFFT) columns have gained approval in civil engineering for different structural applications. A research program is currently being carried out at the laboratories of the Department of Civil Engineering, University of Sherbrooke. The objective of that program is to investigate the compressive behavior of the FRP tube-encased concrete columns. This paper experimentally investigates the performance of the CFFT columns under concentric and eccentric loads. The experimental program was conducted on ten unconfined cylinders, eight CFFT columns. The results were compared to steel spiral reinforcement which have the same confinement pressure of the FRP tubes. The diameter of the FRP tubes was 152 mm and the fibers orientation were mainly in the hoop direction. The results indicated that the behavior of CFFT is affected by the presence of steel bars, laminate thickness and eccentricity load.

Introduction

Fiber reinforced polymer (FRP) composites have been increasingly used in concrete construction. The application of concrete filled FRP tubes (CFFT) technique, such as precast piles, girders, and pier columns [1, 2, 3 and 4]. Several experimental and analytical investigations were conducted to study the behaviors of the CFFT columns. However, most of the research studies were focused on the behavior of CFFT under uniaxial or flexural load. In fact, structural concrete columns under axial loads are exhibited to eccentric load. This occurs for the edge and corner columns in the residential or office building and opened garages. In addition, the designed axially loaded columns can be affected from the eccentricity due to unintentional load eccentricities, possible construction error, lateral deformation and buckling phenomenon. In addition, there are many columns intended to carry an eccentric loads. Therefore, it is important to understand the behavior of the CFFT columns under eccentric load.

Experimental test and analytical model was introduced to describe the behavior of CFFT tubes subjected to combined axial compression loads and bending moment. The study evaluated the confinement as affected by the eccentricity of the applied axial loads as well as the influence of the FRP laminate structure. The results indicated that the interaction curves are significantly affected by both the laminate structure and diameter-to-thickness ratios of the tubes [5]. The behavior of FRP jacketed square concrete columns subjected to eccentric loading was investigated [6]. Nine (108x108x305 mm) square concrete column stubs with zero, one, and two plies of unidirectional carbon FRP fabric were tested under axial loading and various eccentricities. It was concluded that the FRP jacket can greatly enhance the strength and ductility of concrete columns under eccentric loading and that the strain gradient reduces the retrofit efficiency of the FRP jacket for concrete columns. Three different groups of the internally reinforced high strength concrete columns were tested under concentric and eccentric load [7]. Two eccentricities where used (25 and 50 mm), the columns wrapped with two different materials E-glass fiber and carbon fiber. It was concluded that: As the eccentricity was increased the load carrying capacity of the columns was significantly reduced and directly related to the magnitude of eccentricity, a larger eccentricity results in a smaller maximum load. The axial deflection was reduced while the lateral deflection increased with eccentricity.

The objective of this paper is to examine the behavior of CFFT concrete circular columns under concentric and eccentric loading. Ten unconfined cylinders, eight CFFT columns and two control steel spiral reinforcement concrete columns were cast and tested under concentric and eccentric loading. Four CFFT columns loaded with different eccentricity 15, 30, 45 and 60 mm from the center of the columns. An experimental result in term of strengths, lateral and axial deformation, and failure mode was obtained for each column.

Experimental Work

GFRP Tubes

Three types of glass-fiber reinforced polymer GFRP tubes were used. The GFRP tubes were fabricated using filament winding technique; E-glass fiber and Epoxy resin were utilized for manufacturing these tubes. The internal diameter of the tubes is constant and equals 152 mm. Table 1 presents the details for the three types A, B and C of the GFRP tubes, where E_X and E_Y are the Young's modulus in the longitudinal and hoop direc-

tions. The split-disk test and coupon tensile test were performed according to ASTM D-2290-04 and ASTM D 638-03 standard [8, 9], respectively, on five specimens from each type of the tubes. Figure 1 presents the axial tensile stress-strain responses for the three types of the GFRP tube resulted from the coupon tests. Figure 2 shows the average load-strain relationship for each type of the tubes for the split-disk test, and as expected, the highest hoop tensile force values were obtained for the specimens of tube type C which has the largest thickness. In addition, the load-strain curve for the split-disk test was linear up to failure for specimen A and B, however bilinear for tube C.

Concrete Mixes

All specimens were constructed from the same batch of the concrete using a ready mix concrete supplier. The concrete mixture was intended to provide 30 MPa a concrete compressive strength. The materials by kg per m^3 for concrete mixture were 335 cements, 169 water, 331 gravel (aggregate size 2.5-10 mm), 628 gravel (aggregate size 10-20 mm), 856 sand, 70ml/100 kg air-entraining admixture, air content 5-8%, 350ml/100 kg mid-range water reducing admixture (EUCON MRC). Ten plain concrete cylinders (152 x 305 mm) were prepared at the time of casting of CFFT specimens. The average concrete strength at 28-days testing of all cylinders was found to be 30 ± 1 MPa.

Steel Bars

Deformed and mild steel bars No. 10 M and 3.2 mm diameter, respectively, were used to reinforce the CFFT columns and control specimens. Steel bars No. 10 M were used as a longitudinal reinforcement and steel bars 3.2 mm diameter were used as spiral reinforcement for the control specimens. Tensile test for five specimens conducted for each type of the steel bars. The results indicated that the yield tensile strengths were 462 and 675 MPa, also the ultimate tensile strengths were 577 and 820 MPa for steel bars No. 10 M and 3.2 mm diameter, respectively.

Test Matrix and Specimen Preparation

Test matrix and details of the CFFT columns are presented in Table 2. The experimental program for this paper includes four (152 x 912 mm) CFFT and two control specimens subjected to concentric load, also four CFFT columns subjected to variable eccentric load, (15, 30, 45 and 60 mm). The slenderness ratio: height to diameter ratio (H/D) for columns is equal to 6. The CFFT columns were internally reinforced with six deformed steel longitudinal bars 10 M with constant reinforcement ratio equal to 2.60 %, see Figure 3. The bars were distributed uniformly inside the cross section of the GFRP tube. The bars were welded at the top and the bottom of the height by two steel stirrups of 3.2 mm diameter, to fix the bars during casting. The distance between the bars and the tubes was 8 mm. A concrete cover of 10 mm was provided between the ends of the longitudinal steel bars and the top and bottom surfaces of the specimens to avoid the stress concentration at the steel bars area. Finally, the last two specimens in Table 2 present a spirally steel reinforced concrete column. These specimens prepared to be as a control specimen to obtain the ultimate load capacity under a concentric load.

Test Setup and Instrumentation

The specimens were tested under concentric load using a 6,000 kN capacity FORNEY machine as shown in Figure 4. The columns were setup vertically at the center of the loading plates of the machine. However, two rigid steel frames designed and fabricated to test the CFFT specimens under variable eccentric loads. The steel frames placed over the two ends of the CFFT specimens, see Figure 5. Two longitudinal steel rebar, in the tension side of the columns were instrumented at mid height by two electrical resistances strain gages, before casting for each CFFT columns. Also, two axial and two transverse electrical resistances strain gages were mounted 180 degree apart along the hoop direction for each specimen on the external surface of the GFRP tubes at the mid height.

The axial displacement for each column was measured by two linear variable displacement transducers (LVDTs) 180 degrees apart along the hoop direction of the specimen. Moreover, to measure the horizontal displacement, which was expected for all specimens due to the eccentric load, four LVDTs were placed horizontally on the mid-height of the column 90 degrees around the column. The FORNEY machine, strain gages and LVDTs were connected by a 20 channels Data Acquisition System. The data were recorded every one second during the test. The loading rate range was 400 to 600 N/s during the test by manually controlling the loading rate of the hydraulic pump.

Test Results and Discussion

The peak loads (P_r), moment at peak load (M_r), corresponding horizontal displacements at the mid-height of the columns (Δ^*_h), the maximum axial and horizontal deformation (Δ_v) and (Δ_h), respectively, and the confined concrete compressive strength to the unconfined concrete compressive strength ratio (f'_{cc}/f'_c) are given in Table 3.

Figure 6 shows the failure modes for 912 mm height, CFFT columns. The failure of the concentric CFFT columns occurred due to buckling immediately followed by the rupture of the GFRP tube. For CFFT specimens, typical failure was generally recorded by rupture of the GFRP tubes between the one end and the mid-

height of the specimen. All specimens failed in single curvature buckling mode. Distortions of the cross section and outward bulging of the tube near the middle height of the CFFT occurred for all specimens. This resulted from the sliding of the concrete core and local buckling of the internal rebars inside the GFRP tube. Sound snapping was heard even after stopping the test and removal of the specimens from the setup, until the stored energy in the hoop direction and the interaction between fiber and the prestressed concrete core was released.

For eccentrically loaded CFFT columns the failure was generally marked by a ductile failure. Significant decrease in the ultimate load capacity was observed for all eccentrically specimens as compared with the ultimate load capacity of concentrically loaded CFFT columns. Excessive horizontal deformation at the mid height of the CFFT columns was observed beyond the peak load. The final failure mode for the eccentrically loaded CFFT columns was permanent with single curvature buckling in the direction of the tension side. Also, tensile failure in the tension side with minor local buckling in the compression side for the GFRP tube at the mid height occurred for all specimens beyond the peak load due to the increases in the lateral deformations, see Figure 7.

The axial stress- axial and hoop strain relationship for the S-B-00 specimens is bilinear as shown in Figure 8. The average ratios of confined concrete compressive strength to unconfined concrete cylinder strength (f'_{cc}/f'_c) for S-A-00, S-B-00 and S-C-00 are 2.67, 2.93 and 4.30. The axial displacement data were plotted against the axial load for each specimen. To study the effect of thickness and the effect of the confinement, the load-axial deflection curves for CFFT-00 and control column are shown in Figure 9. The ultimate load capacity of the CFFT column was increased by 94 % as compared to the ultimate load capacity of the control specimen. Also a significant improvement in the ductility (axial deformation at the ultimate load) was observed for the CFFT column. Figure 10 shows the axial deformation against the axial load for concentric CFFT columns. It is clear that the ductility of the CFFT columns increased significantly due to the confinement action. In addition, the increase in the ultimate strength increased from 1454 and 1597 to 2323 kN for S-A-00, S-B-00 and S-C-00, respectively. It is clear that by increasing the thickness of the GFRP tube, the ultimate strength of the CFFT columns is increased.

The load-axial deflection curves for the eccentrically loaded CFFT columns are presented in Figure 11. The initial tangent modulus for the eccentrically loaded CFFT columns decreased with increasing the eccentricity values; however the load-deflection curves for these specimens are nonlinear and presented softening response beyond the peak loads opposite to the response of the concentrically column which presented hardening behavior. It was noticed that at the same load level the axial deformation increased with increasing the values of the eccentricity. The largest axial displacement was recorded for S-B-60 which equal to 50 mm. The load-horizontal deflection curves for CFFT columns are plotted in Figure 12. The horizontal deformation for specimen S-B-00 was approximately approached to zero up to load level 80 % of the ultimate load, after that increased to the maximum value at the ultimate load. The lateral deformation of the eccentrically columns increased gradually with load increase up to the peak load, after that the deformation increased progressively with decreasing the load. From Figures 11 and 12, it was observed that the ultimate load capacity of the CFFT columns significantly decreased with the eccentric load and increasing the value of the eccentricity for the same cross section.

Figure 13 shows the relationships between the eccentricity value and the axial load on the CFFT columns. The ultimate load capacity for specimens S-B-15, S-B-30, S-B-45 and S-B-60 decreased 48, 61, 70 and 77 %, respectively as compared to the ultimate load capacity of specimen S-B-00. The experimental results were used to establish interaction diagram for the CFFT columns, see Figure 14. Figure 15 shows the stress-strain curves for S-B-30 specimen. The tension and compression strains are plotted in the left and right side of the figures, respectively. The stress- axial strain curve for the S-B-30 on the compression side presented linear response up to the peak load with the maximum value equal to 0.0007, then descending occurred for the curve with nonlinear response up to failure. In addition, the stress-axial tension strain showed linear response up to 82 % of the peak load with tension-strain equal to .0017, the strain after that increased nonlinearly up to failure, the axial tension strain value at the peak load presented 0.015, this value approximately equal to the yield strain of steel bars. The hoop strain in the compression and tension side showed positive and negative strain values, respectively up to failure.

Conclusions

The behaviors of internally reinforced CFFT columns under concentric and different eccentric load values were presented. The behavior of the concrete filled GFRP tubes is significantly affected by the eccentric load. The test results indicate that by increasing the thickness of the GFRP tubes a significant improvement is achieved in the confinement efficiency. The confinement provided by the GFRP tubes improves both the load-carrying capacity and the ductility of the concrete columns under concentric load. The stress-strain curve of the CFFT tube columns is bilinear and nonlinear for the concentric and eccentric loading, respectively. Increasing the eccentricity values decrease the ultimate load capaci-

ty and increase the horizontal and axial deformation of the CFFT columns.

Acknowledgments:

The research reported in this paper was partially sponsored by the Natural Sciences and Engineering Research Council of Canada (NSERC). The authors also acknowledge the contribution of the Canadian Foundation for Innovation (CFI) for the infrastructure used to conduct testing. Special thanks to the manufacturer (FRE Composites, St-André d'Argenteuil, Qc, Canada) for providing FRP tubes. The opinion and analysis presented in this paper are those of the authors. The technician Nicolas Simard participates in the specimen preparation and testing.

Author(s):

Hamdy Mohamed is a Ph.D. Candidate at the University of Sherbrooke, Sherbrooke, QC, Canada. He received his B.Sc. and M.Sc. degree from the Faculty of Engineering, Helwan University, Egypt in 1999 and 2005, respectively. His research interest is the use of fiber-reinforced polymers (FRP) in reinforced concrete structures. Mohamed is a member of several professional associations including the American Concrete Institute (ACI), the American Society of Civil Engineers (ASCE), the Canadian Society of Civil Engineering (CSCE) and the Egyptian Professional Engineers Association.

Email address:
Hamdy.Mohamed@usherbrooke.ca

Radhouane Masmoudi is a Professor at the University of Sherbrooke, Sherbrooke, QC, Canada. He received his M.Sc. and Ph.D. degree from University of Sherbrooke. His research interests include the development, design, testing and use of fiber-reinforced polymers (FRP) in utility and reinforced concrete structures as well as the finite element modeling of FRP structures. Masmoudi is a member of several professional associations including the American Concrete Institute (ACI), the Canadian Society of Civil Engineering (CSCE) and the Society for the Advancement of Material and Process Engineering (SAMPE).

Email address:
Rahouane.Masmoudi@usherbrooke.ca

References:

1. A. Mirmiran, and M. Shahawy. (2003), "Composite Pile: A Successful Drive." Concrete International, 25, (3), 89-94.

2. A. Fam, M. Pando, G. Filtz, and S. Rizkalla, (2003), "Precast composite piles for the route 40 bridge in virginia using concrete-filled frp tubes" PCI Journal, 48(3), 32-45.

3. A. Fam, R. Green, and S. Rizkalla, (2003), "Field application of Concrete-Filled FRP Tubes for marine piles", ACI Special Publication, SP-215-9, 161-180.

4. V.M. Karbhari, F. Seible, R. Burgueño, A. Davol, M. Wernli, and L. Zhao, (2000), "Structural characterization of fiber-reinforced composite short- and medium-span bridge systems" Applied Composite Material, 7,151–182.

5. A. Fam, B. Flisak, and S. Rizkalla, (2003) "Experimental and Analytical Modeling of Concrete-Filled FRP Tubes Subjected to Combined Bending and Axial Loads" ACI Structural J, Vol. 100, No. 4, pp. 499-509.

6. Z. Parvinl, and W. Wang, (2001) "Behavior of FRP jacketed concrete columns Under Eccentric Loading" Journal of Composites for Construction, Vol. 5, No. 3, pp. 146-152.

7. MNS. Hadi, (2007), "Behaviour of FRP strengthened concrete columns under eccentric compression loading", J Comp Struct, Vol. 77, pp. 92–96.

8. ASTM D2290-04 Standard Test Method for Apparent Hoop Tensile Strength of Plastic or Reinforced Plastic Pipe by Split Disk Method.

9. ASTM D638-03 Standard Test Method for Tensile Properties of Plastics.

Table 1: Dimension and mechanical properties of fiber reinforced polymer tubes

Tube type	Internal diameter (mm)	Thickness (mm)	Number of layers	Stacking sequence	E_X (MPa)	E_Y (MPa)
A	152	2.65	6	$[\pm 60^o]_3$	8785	20690
B	152	2.70	8	$[\pm 60^o]_4$	8787	20860
C	152	6.40	14	$[\pm 65_3, \pm 45, \pm 65_3]$	9270	23630

Table 2: Details of specimens and summary of test matrix

Specimen ID	Height (mm)	Eccentricity (e=mm)	Internal reinforcement	Loading pattern	Type of confinement
S-A-00		0	6 No. 10	Concentric	GFRP Tube
S-B-00		0	6 No. 10	Concentric	GFRP Tube
S-C-00		0	6 No. 10	Concentric	GFRP Tube
S-B-15		15	6 No. 10	Eccentric	GFRP Tube
S-B-30	912	30	6 No. 10	Eccentric	GFRP Tube
S-B-45		45	6 No. 10	Eccentric	GFRP Tube
S-B-60		60	6 No. 10	Eccentric	GFRP Tube
Control-1		0	6 No. 10	Concentric	Steel Spiral
Control-2		0	6 No. 10	Concentric	Steel Spiral

Table 3: Summary of test results.

Specimen ID	P_r(kN)	Δ_h(mm) Maximum	Δ_v(mm) Maximum	Δ^*_h(mm)	M_r (kN.m)	(f'_{cc}/f'_c)
S-A-00	1454	62.00	35.00	----	00	2.67
S-B-00	1595	73.70	32.05	----	00	2.93
S-C-00	2323	07.20	38.00	----	00	4.30
S-B-15	825.0	81.00	28.33	31.00	25.51	1.51
S-B-30	620.0	117.0	39.10	45.5	28.00	1.14
S-B-45	466.0	97.00	43.2	60.00	27.84	0.85
S-B-60	367.0	118.00	50.00	73.00	26.72	0.67
Control	822.0	2.00	4.40	----	0	1.50

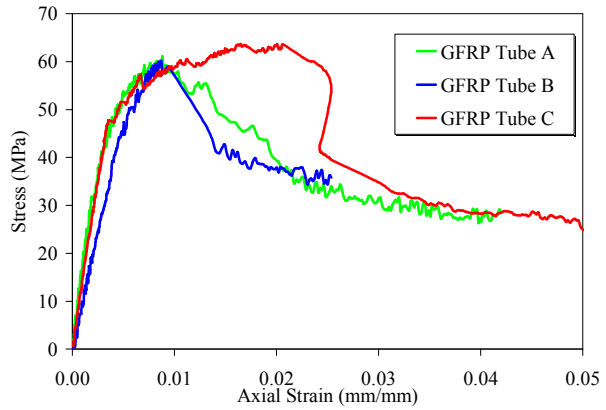

Figure 1: Stress-strain curve for coupon tensile test

Figure 3.b: Setup of rebars cages for CFFT columns

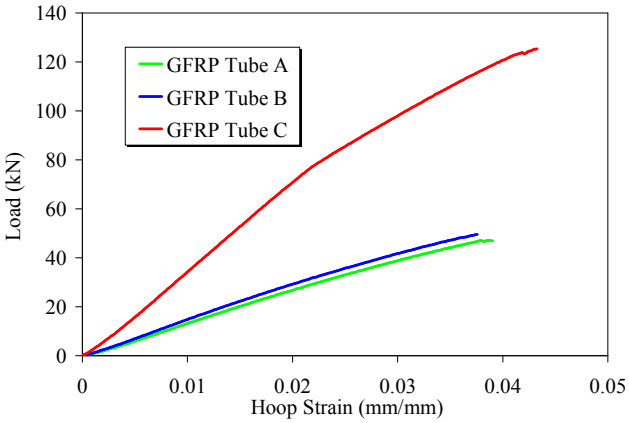

Figure 2: Load-strain curve for the split-disk

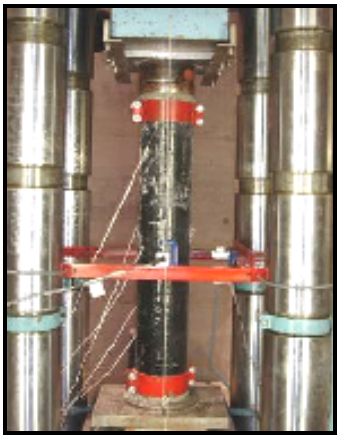

Figure 4: Test setup (concentric load)

Figure 3.a: 152 x 912 mm GFRP Tube-columns

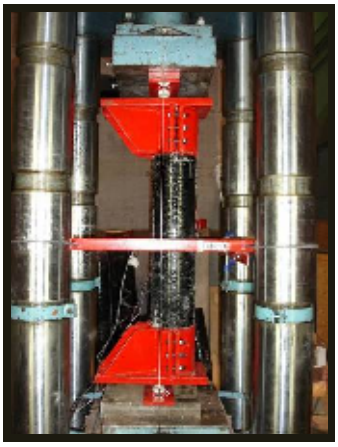

Figure 5: Test setup (eccentric loads)

Figure 6: Failure mode of the concentric columns

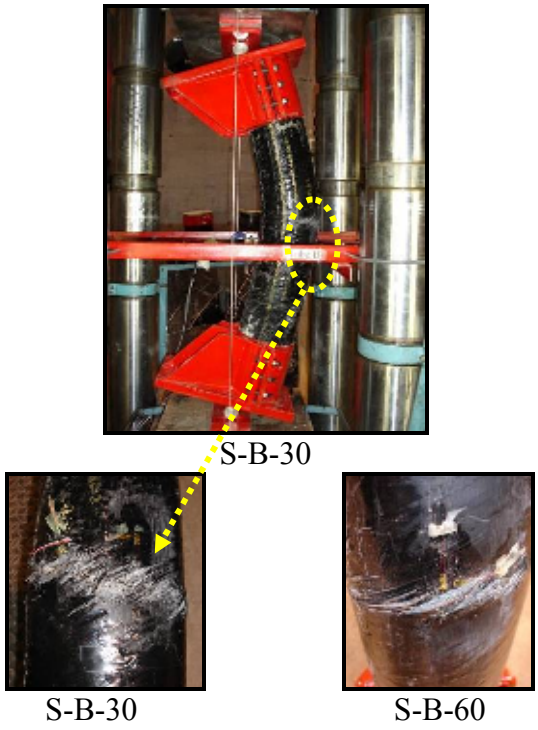

Figure 7: Failure mode of the eccentric columns

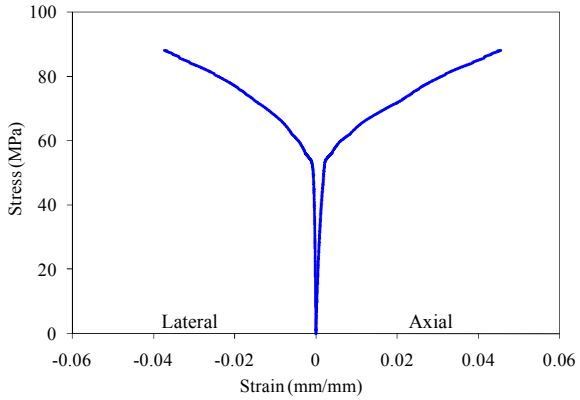

Figure 8: Stress-strain relationships for S-B-00

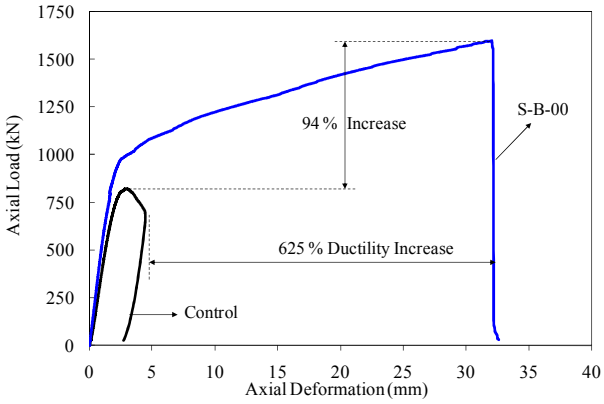

Figure 9: Load-axial deformation relationships

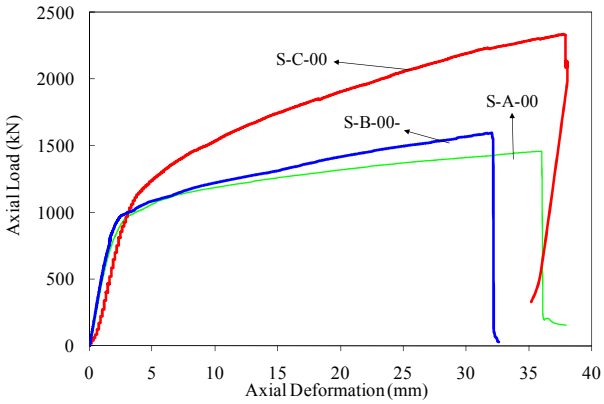

Figure 10: Load-axial deformation relationships

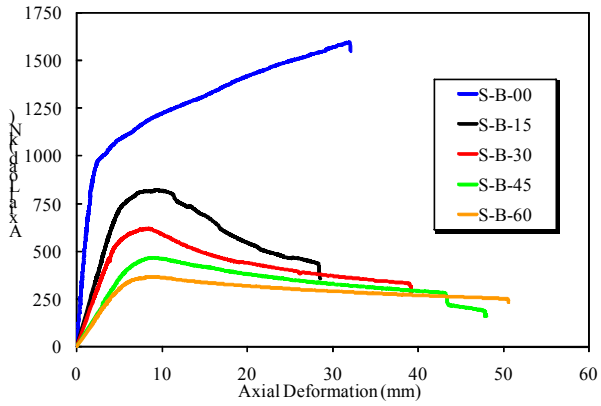

Figure 11: Load-axial deformation relationships

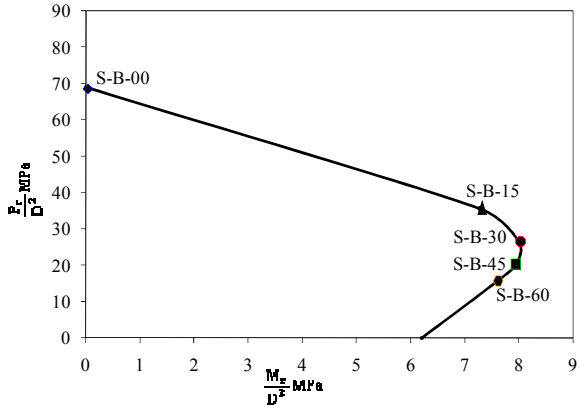

Figure 14:. Interaction diagram for CFFT columns

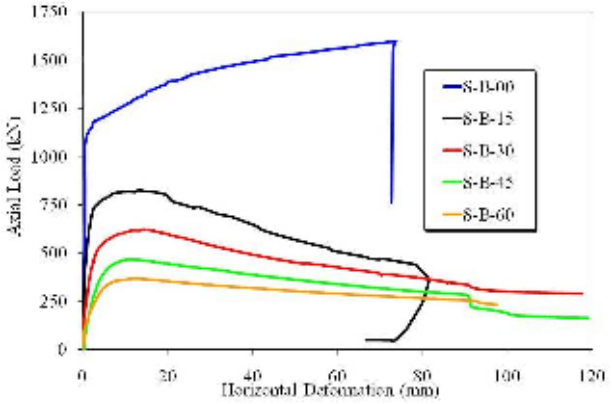

Figure 12: Load-lateral deformation relationships

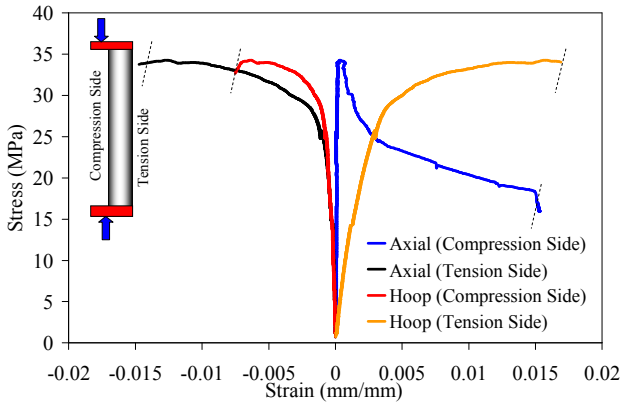

Figure 15: Stress-strain relationships for S-B-30

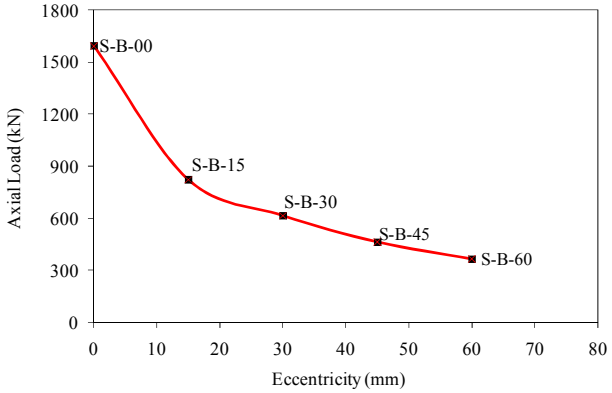

Figure 13: Load-Eccentricity relationships